Diphosphine as an Overhead Bridge across a Heterometallic M−M′ Bond. A Flexible Cluster System in (P−P)$AuMn_2(CO)_7(\mu$-$PPh_2)$ that Accommodates All Common Diphosphines

Kim Hun Lee, Pauline M. N. Low, and T. S. Andy Hor*

Department of Chemistry, Faculty of Science, National University of Singapore, Kent Ridge, Singapore, 119260

Yuh-Sheng Wen and Ling Kang Liu

Institute of Chemistry, Academia Sinica, Taipei 11529, Taiwan, Republic of China

Received January 22, 2001

The inter-triangular diphosphine bridge in $[AuMn_2(CO)_8(\mu$-$PPh_2)]_2(\mu$-P−P) turns into an intra-triangular one as it undergoes amine-oxide-promoted decarbonylation to give (P−P)-$AuMn_2(CO)_7(\mu$-$PPh_2)$ (P−P = Ph_2P−X−PPh_2; X = $(CH_2)_n$, $Fe(C_5H_4)_2$; n = 1−4) in the presence of the corresponding free diphosphine. The resultant triangular cluster contains a heterometallic Au−Mn bond overbridged by all common diphosphines attempted, including dppf (X = $Fe(C_5H_4)_2$) and dppp (n = 3). The Au−Mn bond supported by dppf (2.6797(7) Å) is shorter than that supported by dppe (n = 2) (2.756(2) Å) or dppp (2.7643(4) Å).

Introduction

A key interest in heterometallic systems stems from its unique ability to bring together entities of fundamentally different electronic properties.[1] In proximity, they preserve their inherent characteristics, yet develop new traits that are dependent on the heterometallic system.[2] This is a basic incentive that brought about the upheaval of heterometallic chemistry, especially in bimetallic catalysis,[3] bifunctional polymers,[4] soluble alloys,[5] etc. One difficulty facing this line of chemistry is the weakness of many (not all) M−M′ bonds, especially in solution.[6] The rupture of these bonds destroys the underlying principle in using heterometallics as substrates. In this note, using $[AuMn_2(CO)_8(\mu$-$PPh_2)]_2$-(μ-P−P) (P−P = diphosphine),[7] **1**, as a model, we report a simple yet effective strategy to preserve the M−M′ entity, by protecting it with an overhead bridge. We opt for a diphosphine because of its convenience and its ability to bind to a range of metals. Surprisingly however, there are very few documented systems where the M−M′ bond can be stabilized by diphosphines. For the few that are reported,[8] it is rare to have a system that can sustain a range of common diphosphines of different steric and geometric demand. This can be traced to the sensitive dependence of complex stability on the M−M′ length, which in turn is influenced by the overhead bridge stereogeometry. The present system is robust and sustainable by all common diphosphines that we have studied.

Results and Discussion

Complexes **1a** (P−P = $Fe(C_5H_4PPh_2)_2$ (dppf)) and **1d** (P−P = $Ph_2P(CH_2)_2PPh_2$ (dppe)), which were a subject of our earlier report,[7] are examples of complexes with two heterometallic triangles linked exclusively by a diphosphine bridge, giving a hexametallic framework. The other derivatives, **1b** (P−P = $Ph_2P(CH_2)_4PPh_2$ (dppb)), **1c** (P−P = $Ph_2P(CH_2)_3PPh_2$ (dppp)), and **1e** (P−P = $Ph_2PCH_2PPh_2$ (dppm)), can also be prepared accordingly. Me_3NO-induced decarbonylation of **1** in the presence of the corresponding free diphosphine P−P afforded (P−P)$AuMn_2(CO)_7(\mu$-$PPh_2)$ (P−P = dppf (**2a**), dppb (**2b**), dppp (**2c**), dppe (**2d**), dppm (**2e**)). IR analysis is consistent with the loss of CO, whereas the ^{31}P NMR spectra invariably show three discrete resonances corresponding to the phosphines on Au (P_{Au}) and Mn (P_{Mn}) and the phosphide (P_{Ph}) bridge. These point to isostructural products regardless of the diphosphine used. The neighboring ^{55}Mn quadrupolar nucleus has broadened the P_{Mn} and P_{Ph} signals, which renders any coupling

* To whom correspondence should be addressed.

(1) (a) González, B.; Cuadrado, I.; Casado, C. M.; Alonso, B.; Pastor, C. J. *Organometallics* **2000**, *19*, 5518. (b) Zhang, C.; Guzei, I. A.; Espenson, J. H. *Organometallics* **2000**, *19*, 5257. (c) Komine, N.; Hoh, H.; Hirano, M.; Komiya, S. *Organometallics* **2000**, *19*, 25, 5251.

(2) (a) Fukuoka, A.; Saigiura, T.; Yasuda, T.; Taguchi, T.; Hirano, M.; Komiya, S. *Chem. Lett.* **1997**, 329. (b) Fukuoka, A.; Fukagawa, S.; Hirano, M.; Komiya, S. *Chem. Lett.* **1997**, 377.

(3) Fukuoku, A.; Sadashima, T.; Sugiura, T.; Wu, X.; Mizuho, Y.; Komiya, S. *J. Organomet. Chem.* **1994**, *473*, 139.

(4) Cottone, A. III; Scott, M. J. *Organometallics* **2000**, *19*, 5254.

(5) Zhang, J.; Zhang, Y.-H.; Chen, X.-N.; Ding, E.-R.; Yin, Y. Q. *Organometallics* **2000**, *19*, 5032.

(6) (a) Zhang, Y.; Sun, X.; Wang, B.; Xu, S.; Zhou, X. *Organmetallics* **1999**, *18*, 4493. (b) Tanaka, K. *Bull. Chem. Soc. Jpn.* **1998**, *71*, 17.

(7) Low, P. M. N.; Tan, A. G.; Hor, T. S. A. *Organometallics* **1996**, *15*, 2595.

(8) (a) Housecroft, C. E.; Rheingold A. L.; Waller, A.; Yap, G. P. A. *J. Organomet. Chem.* **1998**, *565*, 105. (b) Hattersley, A. D.; Housecroft, C. E.; Rheingold, A. L. *Inorg. Chim. Acta* **1999**, *289*, 149. (c) Braunstein, P.; de Méric de Bellefon, C.; Oswald, B.; Ries, M.; Lanfranchi, M.; Tiripicchio, A. *Inorg. Chem.* **1993**, *32*, 1638. (d) Braunstein, P.; de Méric de Bellefon, C.; Oswald, B. *Inorg. Chem.* **1993**, *32*, 1649. (e) Barkley, J. V.; Grimshaw, J. C.; Higgins, S. J.; Hoare, P. B.; McCart, M. K.; Smith, A. K. *J. Chem. Soc., Dalton Trans.* **1995**, 2901.

10.1021/om0100434 CCC: $20.00
Publication on Web 06/21/2001

Scheme 1. Proposed Mechanistic Pathway for the Formation of 2 from 1 in the Presence of the Corresponding Free Diphosphine

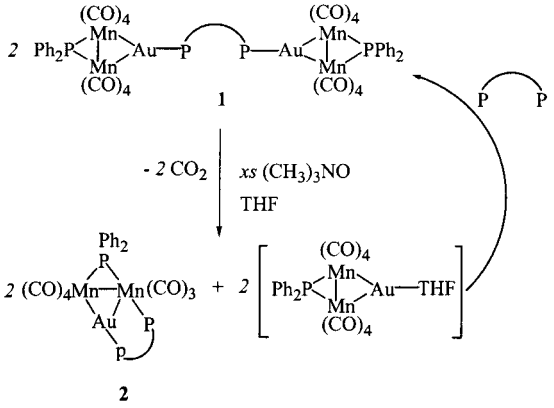

unrecognizable. Coupling between P_{Au} and P_{Mn} is only observed for short-chain diphosphines and is strongest in the case of dppm (15, 38, and 124 Hz in **2c**, **2d**, and **2e**, respectively). This supports the formation of a new heterometallic triangle, with formal Mn−Mn and Au−Mn bonds, that is supported by a phosphide-bridged Mn−Mn bond and a diphosphine bridge over the two heterometals. $P_{Mn}-P_{Au}$ coupling occurs across the alkyl chain of the phosphine instead of the Au−Mn bond. The formation mechanism likely involves decarbonylation, which triggers a swing of the diphosphine from an inter-triangular to an intra-triangular bridging mode and an unsaturated intermediate $(THF)AuMn_2(CO)_8(\mu\text{-}PPh_2)$ (Scheme 1). This may be preceded by the formation of another intermediate, $AuMn_2(CO)_7(THF)(\mu\text{-}PPh_2)(\eta^1\text{-}P-P)$. The unsaturated Au site of $(THF)AuMn_2(CO)_8(\mu\text{-}PPh_2)$ is then satisfied by the incoming free diphosphine. If the reaction is carried out in the absence of a free diphosphine, the yield is inevitably lower, although the decarbonylation product can still be isolated. If **1** is mixed with a diphosphine that does not correspond to that in **1**, two sets of product mixtures would result; for example, **1a** and free dppe would give a mixture containing **1a**, **2a**, **1d**, and **2d**. This are consistent with the formation mechanism depicted in Scheme 1. There is no evidence for any fluxional behavior on the NMR time scale, e.g., phosphine bridge flipping across two Mn sites by exchanging with a carbonyl.

Instead, with our interest in the M−M′ bonding properties in the presence of an overhead diphosphine bridge and because it is rare to see a heterometal−metal bond that can accommodate a wide range of diphosphines without undergoing structural changes, we have opted to carry out the X-ray single-crystal structural determination of **2a**, **2c**, and **2d** (Figure 1 (**2a**), Figure 2 (**2c**), and Figure 3 (**2d**) and Table 2 (**2a**, **2c**, **2d**)). The results are in agreement with the solution structures proposed. The M−M′ bond data revealed a few unexpected features: (1) When a M−M bond is overbridged by a diphosphine, and especially if the diphosphine has a strict stereoconformational demand, the M−M bond is expected to lengthen and is presumably weakened. This is observed in **2c** and **2d** but not in **2a**, where the two Au−Mn lengths are not significantly different. (2) Dppf is known to form a range of bridging and chelate complexes.[9] It is therefore not suitable to bridge metals that are directly and formally connected, for obvious steric and conformation reasons. There are only a few notable exceptions[10] among a vast number of dppf

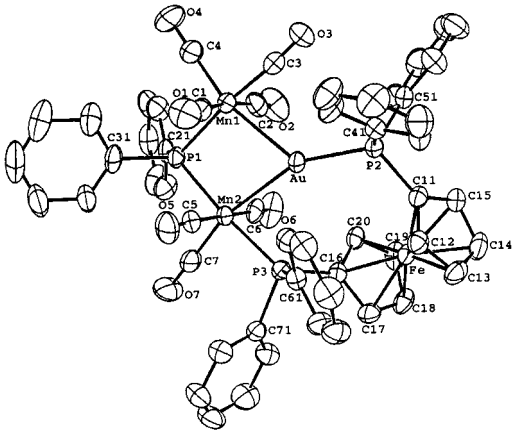

Figure 1. ORTEP plot (50% ellipsoids) of the molecular structure of **2a**.

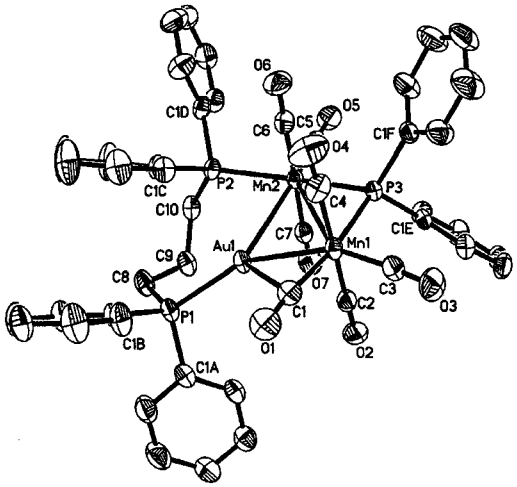

Figure 2. ORTEP plot (50% ellipsoids) of the molecular structure of **2c**.

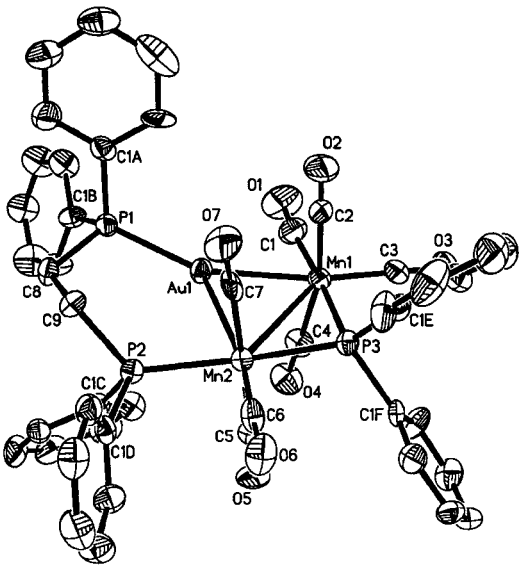

Figure 3. ORTEP plot (50% ellipsoids) of the molecular structure of **2d**.

(9) Gan, K.-S.; Hor, T. S. A. In *Ferrocenes−Homogeneous Catalysis, Organic Synthesis and Materials Science*; Togni, A., Hayashi, T., Eds.; VCH: Weinheim, 1995; p 3.

Table 1. Crystallographic Data for (P−P)AuMn$_2$(CO)$_7$(μ-PPh$_2$), the dppf, 2a, dppp, 2c, and dppe Derivative, 2d

	2a	2c	2d
chemical formula	$C_{53}H_{38}AuFeMn_2O_7P_3$	$C_{46}H_{36}AuMn_2O_7P_3$	$C_{45}H_{34}AuMn_2O_7P_3$
fw	1242.48	1100.50	1086.48
cryst syst	triclinic	monoclinic	monoclinic
space group	$P\bar{1}$	$P2_1/c$	$P2_1/n$
a, Å	10.7650(11)	15.4238(2)	12.6824(2)
b, Å	13.9796(15)	16.7258(1)	16.2029(1)
c, Å	17.2151(17)	17.670(3)	20.7343(3)
α, deg	110.014(9)	90	90
β, deg	97.429(1)	108.8210(10)	91.9710(10)
γ, deg	93.908(1)	90	90
V, Å^3	2396.2(4)	4314.69(6)	4258.21(9)
Z	2	4	4
ρ_{cacld}, g cm^{-3}	1.722	1.694	1.695
μ, mm^{-1}	3.984	4.130	4.184
temp (K)	295	223 (2)	223 (2)
no. of rflns collected	8749	26 829	20 607
no. of ind rflns	8443	10 634 [R(int) = 0.0276	7391 [R(int) = 0.0819]
no. of params	604	522	523
GOF	1.34	1.018	1.073
R_1 and wR_2 (obsd data)[a,b]	0.028 and 0.030	0.0283 and 0.0619	0.0737 and 0.1849

[a] $R_1 = ||F_o| - |F_c||/|F_o|$. [b] $wR_2 = \{w[(F_o^2 - F_c^2)^2]/w[(F_o^2)^2]\}$, $w^{-1} = \sigma^2(F_o^2) + (aP)^2 + bP$.

complexes known today.[11] Not only is **2a** a rare exception to this rule, it also shows an exceptional quality among this series that the dppf-bridged Au−Mn bond is only marginally longer than its unbridged counterpart. This is an encouraging sign for the use of dppf in supporting clusters and heterometallic species as catalytic precursors. (3) When options are available, dppp would prefer its coordination mode to be chelating or bridging metals that are not bonded.[12] Complex **2c** is another rare exception. Its ability to stabilize a M−M entity, albeit with a longer M−M bond, is exemplified in the isolation of **2c**. (4) Although dppe has the shortest carbon backbone, the Au−Mn bond in **2d** is not the shortest and is in fact significantly longer than that in **2a**. The weakness of the Mn−Mn bond such as in **2a**, **2c**, and **2d** (3.1485(9), 3.1167(6), and 3.134(2) Å, respectively) has been discussed in our earlier paper.[7] Complex **2c** shows a unique feature in its carbonyl data. One terminal CO is semibridged to Au (Au−C(1) = 2.616(3) Å), supported by its absorbance in the IR region (1893 cm^{-1}). The Mn−C(CO) bonds of those CO's, which are trans to Au (av = 1.777(5) Å, **2a**; 1.787(3) Å, **2c**; 1.789(12) Å, **2d**) are shorter than those of other CO's (av = 1.833(5) Å, **2a**; 1.838(3) Å, **2c**; 1.853(13) Å, **2d**). They are seemingly lengthened from **2a** to **2c** and to **2d**. This structural parameter suggests that the Mn−C(CO) bonds are weakened upon increasing the steric bulkiness of the diphosphine.

We have an unusual example that shows that a heterometallic cluster can remain isostructural with different types of diphosphines over its key entity, the M−M′ bond. The complex has a self-adapting and self-stabilizing mechanism simply by adjusting its M−M′ lengths, among others, without sacrificing its stability. This is a simple idea but surprisingly has eluded many reports in the heterometallic literature. Complex **2a** is stable toward CO and PPh_3 addition, although it can be destroyed by $PPhMe_2$. Its unexpected chemical stability and the M−M′ bonding features prompted us to reassess the ability of dppf to support a M−M bond in general and, in particular, the strategy in the use of dppf complexes in bimetallic catalysis. We have reviewed the value of dppf as a promoter in a range of catalytic processes.[9] This finding gives us confidence that the search for heterometallics as bimetallic catalysts can be realized. A suitable candidate can be one that is stabilized by dppf over a formal M−M′ bond, which, upon entry of substrate, can convert to other common coordination modes. This ability of diphosphines to switch bonding modes comfortably, without destroying the complex and thereby disrupting complex behavior, is a key in this line of investigation.

Experimental Section

General Procedure. All reactions were performed under purified nitrogen using standard Schlenk techniques. Solvents used were of reagent grade and were freshly distilled and degassed under purified nitrogen before use. Precoated silica TLC plates of 0.25 mm layer thickness were obtained from Merck or Baker. All IR spectra were recorded on a Perkin-Elmer 1600 FT-IR spectrometer. ^{1}H and ^{31}P NMR spectra were recorded in $CDCl_3$ solution on a Bruker ACF 300 MHz spectrometer at ca. 300 K at field strengths of 300.0 and 121.5 MHz, respectively. ^{1}H and ^{31}P chemical shifts are quoted in ppm downfield of Me_4Si and externally referenced to 85% H_3PO_4, respectively. Elemental analyses were carried out in the Chemistry Department of the National University of Singapore (NUS). When solvate of crystallization is present, it was verified by ^{1}H NMR analysis.

X-ray Crystallography. The diffraction experiments for the samples **2c** and **2d** were carried out on a Bruker AXS CCD diffractometer with a Mo Kα sealed tube at −50 °C. The program SMART[13] was used for collection of data frames, indexing reflection, and determination of lattice parameters,

(10) (a) Yeo, J. S. L.; Li, G.; Yip, W.-H.; Handerson, W.; Mak, T. C. W.; Hor, T. S. A. *J. Chem. Soc., Dalton Trans.* **1999**, 435. (b) Canales, F.; Gimeno, M. C.; Laguna, A.; Jones, P. G. *J. Am. Chem. Soc.* **1996**, *118*, 4839. (c) Calhorda, M. J.; Canales, F.; Gimeno, M. C.; Jiménez, J.; Jones, P. G.; Laguna, A.; Veiros, L. F. *Organometallics* **1997**, *16*, 3837. (d) Canales, F.; Gimeno, M. C.; Laguna, A.; Jones, P. G. *Organometallics* **1996**, *15*, 3412.

(11) (a) Bandoli, G.; Dolmella, A. *Coord. Chem. Rev.* **2000**, *209*, 161, and references therein. (b) Fong, S.-W. A.; Hor, T. S. A. *J. Cluster Sci.* **1998**, *9*, 351, and references therein.

(12) (a) Macías, R.; Rath, N. P.; Barton, L. *Organometallics* **1999**, *18*, 3637. (b) Ferrer, M.; Rossell, O.; Seco, M.; Soler, M.; Font-Bardía, M.; Solans, X.; de Montauzon, D. *J. Organomet. Chem.* **2000**, *598*, 215. (c) Ferrer, M.; Julià, A.; Reina, R.; Rossell, O.; Seco, M.; de Montauzon, D. *J. Organomet. Chem.* **1998**, *560*, 147. (d) Goldberg, J. E.; Mullica, D. F.; Sappenfield, E. L.; Stone, G. A. *J. Chem. Soc., Dalton Trans.* **1992**, 2495.

Table 2. Selected Bond Lengths (Å) and Bond Angles (deg) for (P−P)AuMn$_2$(CO)$_7$(μ-PPh$_2$)

2a			
Au−Mn(1)	2.6655(7)	Au−Mn(2)	2.6797(7)
Mn(1)−Mn(2)	3.1485(9)	Au−P(2)	2.3356(12)
Mn(1)−P(1)	2.2797(14)	Mn(2)−P(1)	2.2701(13)
Mn(2)−P(3)	2.3366(13)	Mn(1)−C(1)	1.833(5)
Mn(1)−C(2)	1.846(6)	Mn(1)−C(3)	1.830(5)
Mn(1)−C(4)	1.783(5)	Mn(2)−C(5)	1.820(5)
Mn(2)−C(6)	1.834(5)	Mn(2)−C(7)	1.770(5)
mean Fe−C	2.051(5)	mean C−O (1−4)	1.143(7)
mean C−O (5−7)	1.153(7)		
Mn(1)−Au−Mn(2)	72.178(21)	Au−Mn(2)−Mn(1)	53.702(18)
Au−Mn(1)−Mn(2)	54.119(18)	Mn(1)−P(1)−Mn(2)	87.58(5)
Mn(2)−Mn(1)−P(1)	46.08(3)	Mn(1)−Mn(2)−P(1)	46.34(3)
Mn(1)−Au−P(2)	132.08(3)	Mn(2)−Au−P(2)	155.73(3)
Au−Mn(1)−P(1)	100.08(4)	Au−Mn(2)−P(1)	99.92(4)
Au−Mn(2)−P(3)	73.30(3)	Au−Mn(1)−C(1)	85.97(15)
Au−Mn(1)−C(2)	85.24(16)	Au−Mn(1)−C(3)	73.32(14)
Au−Mn(1)−C(4)	164.10(17)	Au−Mn(2)−C(5)	94.75(15)
Au−Mn(2)−C(6)	86.99(15)	Au−Mn(2)−C(7)	164.88(15)
P(1)−Mn(2)−P(3)	172.63(5)	Mn(1)−Mn(2)−P(3)	126.64(4)
Mn(1)−C(1)−O(1)	177.4(5)	Mn(1)−C(2)−O(2)	179.1(5)
Mn(1)−C(3)−O(3)	174.1(4)	Mn(1)−C(4)−O(4)	177.3(5)
Mn(2)−C(5)−O(5)	176.3(4)	Mn(2)−C(6)−O(6)	175.4(5)
Mn(2)−C(7)−O(7)	178.0(4)	Mn(2)−P(3)−C(16)	119.57(15)
Mn(2)−P(3)−C(61)	122.5(14)	Mn(2)−P(3)−C(71)	106.87(14)
2c			
Au−Mn(1)	2.6416(4)	Au−Mn(2)	2.7643(4)
Mn(1)−Mn(2)	3.1167(6)	Au−P(1)	2.3177(8)
Mn(1)−P(3)	2.3022(8)	Mn(2)−P(3)	2.2534(8)
Mn(2)−P(2)	2.3048(8)	Mn(1)−C(1)	1.812(3)
Mn(1)−C(2)	1.834(3)	Mn(1)−C(3)	1.793(3)
Mn(1)−C(4)	1.855(4)	Mn(2)−C(5)	1.780(3)
Mn(2)−C(6)	1.848(3)	Mn(2)−C(7)	1.842(3)
mean C−O (1−4)	1.151(4)	mean C−O (5−7)	1.148(4)
Mn(1)−Au−Mn(2)	70.373(13)	Au−Mn(1)−Mn(2)	56.658(11)
Mn(1)−Mn(2)−Au	52.969(11)	Mn(1)−P(3)−Mn(2)	86.33(3)
P(3)−Mn(1)−Mn(2)	46.18(2)	Mn(1)−Mn(2)−P(3)	47.79(2)
P(2)−Mn(2)−P(3)	170.02(3)	P(2)−Mn(2)−Mn(1)	124.07(2)
Mn(2)−Au−P(1)	136.55(2)	Mn(1)−Au−P(1)	152.03(2)
Au−Mn(2)−P(3)	98.90(2)	Au−Mn(1)−P(3)	101.23(2)
Au−Mn(1)−C(1)	69.08(10)	Au−Mn(2)−P(2)	74.58(2)
Au−Mn(1)−C(3)	156.45(11)	Au−Mn(1)−C(2)	76.90(9)
Au−Mn(2)−C(5)	157.39(10)	Au−Mn(1)−C(4)	99.75(11)
Au−Mn(2)−C(7)	75.12(9)	Au−Mn(2)−C(6)	105.40(10)
Mn(1)−C(2)−O(2)	177.7(3)	Mn(1)−C(1)−O(1)	171.4(3)
Mn(1)−C(4)−O(4)	177.2(3)	Mn(1)−C(3)−O(3)	175.8(3)
Mn(2)−C(6)−O(6)	175.8(3)	Mn(2)−C(5)−O(5)	177.1(3)
Mn(2)−P(2)−C(1C)	121.79(10)	Mn(2)−C(7)−O(7)	175.0(3)
Mn(2)−P(2)−C(10)	116.77(10)	Mn(2)−P(2)−C(1D)	111.81(10)
2d			
Au−Mn(1)	2.601(2)	Au−Mn(2)	2.756(2)
Mn(1)−Mn(2)	3.134(2)	Au−P(1)	2.301(3)
Mn(1)−P(3)	2.292(3)	Mn(2)−P(3)	2.243(3)
Mn(2)−P(2)	2.311(3)	Mn(1)−C(1)	1.817(14)
Mn(1)−C(2)	1.857(14)	Mn(1)−C(3)	1.794(12)
Mn(1)−C(4)	1.836(12)	Mn(2)−C(5)	1.877(12)
Mn(2)−C(6)	1.784(12)	Mn(2)−C(7)	1.880(12)
mean C−O (1−4)	1.141(16)	mean C−O (5−7)	1.117(14)
Mn(1)−Au−Mn(2)	71.55(5)	Au−Mn(1)−Mn(2)	56.52(4)
Mn(1)−Mn(2)−Au	51.93(4)	Mn(1)−P(3)−Mn(2)	87.41(11)
P(3)−Mn(1)−Mn(2)	45.65(8)	Mn(1)−Mn(2)−P(3)	46.94(8)
P(2)−Mn(2)−P(3)	171.09(12)	P(2)−Mn(2)−Mn(1)	124.66(9)
Mn(2)−Au−P(1)	128.04(8)	Mn(1)−Au−P(1)	157.05(8)
Au−Mn(2)−P(3)	98.29(9)	Au−Mn(1)−P(3)	101.57(9)
Au−Mn(1)−C(1)	73.6(4)	Au−Mn(2)−P(2)	73.97(8)
Au−Mn(1)−C(3)	166.6(4)	Au−Mn(1)−C(2)	83.2(4)
Au−Mn(2)−C(5)	104.7(4)	Au−Mn(1)−C(4)	83.3(4)
Au−Mn(2)−C(7)	78.2(4)	Au−Mn(2)−C(6)	165.3(4)
Mn(1)−C(2)−O(2)	178.1(12)	Mn(1)−C(1)−O(1)	173.5(13)
Mn(1)−C(4)−O(4)	176.7(11)	Mn(1)−C(3)−O(3)	179.2(13)
Mn(2)−C(6)−O(6)	178.6(10)	Mn(2)−C(5)−O(5)	174.4(11)
Mn(2)−P(2)−C(1C)	120.6(4)	Mn(2)−C(7)−O(7)	173.9(13)
Mn(2)−P(2)−C(9)	123.6(4)	Mn(2)−P(2)−C(1D)	106.1(3)

SAINT[13] for integration of intensity of reflection and scaling, SADABS[14] for absorption correction, and SHELXTL[15] for space group and structure determination and refinements. The data collection of the compound **2a** was done on a Nonius diffractometer with scintillation counter and a Mo Kα sealed tube at 22 °C. Crystal data and refinement details are given in Table 1.

Electrospray Mass Spectrometry (ESMS). ES spectra were recorded in both positive- and negative-ion mode on a Finnigan LCQ spectrometer. The spray voltage was 4.5 kV, and the capillary temperature was 70 °C. Identification of all major bands was achieved by comparison of experimental and calculated isotope distribution patterns; the latter were obtained using the ISOTOPE simulation program. Samples were dissolved in a minimum amount of THF and diluted with sodium methoxide. Only the molecular ions are reported below.

Preparation of [AuMn$_2$(CO)$_8$(μ-PPh$_2$)]$_2$(μ-P−P) (1a, 1b, 1c, 1d, 1e). 1a and **1d** were prepared using our reported method.[7] **1b**, **1c**, and **1e**, which have not been reported, were similarly prepared. The products, upon purification by column chromatography, were used directly in the subsequent decarbonylation reaction. ^{31}P NMR (δ) for **1b**: 59.81 (s, P$_{Au}$); 214.66 (s, br, PPh$_2$); for **1c**: 58.46 (s, P$_{Au}$); 215.32 (s, br, PPh$_2$); for **1e**: 57.96 (s, P$_{Au}$); 213.72 (s, br, PPh$_2$).

Synthesis of (P−P)AuMn$_2$(CO)$_7$(μ-PPh$_2$) (2a). Me$_3$NO (0.0278 g, 0.25 mmol) was added to a stirred solution of complex **1a** (0.0993 g, 0.05 mmol) and dppf (0.0282 g, 0.05 mmol) in THF (25 mL). The mixture slowly turned from orange to red. After 4 h, the red mixture was stripped of solvent and the red residue was redissolved in a minimum amount of CH_2Cl_2. Development on silica TLC plates upon elution with CH_2Cl_2/hexane (2:3) gave two bands: band 1 (orange, **1a**, 0.0062 g, 6%) and band 2 (red, **2a**, 0.0596 g, 48%). Anal. Calcd for **2a**: C, 51.23; H, 3.08. Found: C, 51.00; H, 3.10. ESMS: [**2a** + Na]$^+$ (*m*/*z* 1264.5). ^{1}H NMR (δ): 4.43 (m, CpH$_\alpha$, 4H); 4.99 (m, CpH$_\beta$, 4H); 7.21−7.24 (m, Ph, 13H); 7.47 (m, Ph, 7H); 7.63−7.67 (m, Ph, 5H); 7.83−7.89 (m, Ph, 5H). ^{31}P NMR (δ): 64.21 (s, P$_{Au}$); 74.16 (s, br, P$_{Mn}$); 214.13 (s, br, PPh$_2$). IR (CO, cm^{-1}): 2040 s, 1991 s, 1974 s, 1942 vs, 1934 sh, 1913 s, 1899 s (solid KBr).

Synthesis of (P−P)AuMn$_2$(CO)$_7$(μ-PPh$_2$) (2b). Similar preparation from Me$_3$NO (0.0278 g, 0.25 mmol), **1b** (0.0929 g, 0.05 mmol), and dppb (0.0213 g, 0.05 mmol) in THF (25 mL) at 50 °C for 4.5 h gave two bands: band 1 (orange, **1b**, 0.0074 g, 8%) and band 2 (red, **2b**·1/4CH_2Cl_2, 0.0390 g, 34%), after elution with CH_2Cl_2/hexane (1:1). Anal. Calcd for **2b**·1/4CH_2Cl_2: C, 49.97; H, 3.42. Found: C, 49.83; H, 4.22. ESMS: [**2b** + Na]$^+$ (*m*/*z* 1136.6). ^{1}H NMR (δ): 1.37−1.44 (m, CH$_2$, 2H); 2.22 (m, CH$_2$, 2H), 2.54−2.62 (m, CH$_2$, 2H); 2.95−3.20 (m, CH$_2$, 2H); 5.27 (s, CH_2Cl_2, 0.5H); 7.18−7.25 (m, Ph, 8H); 7.42−7.60 (m, Ph, 18H), 7.73−7.91 (m, Ph, 4H). ^{31}P NMR (δ): 54.22 (s, P$_{Au}$); 75.42 (s, br, P$_{Mn}$); 207.35 (s, br, PPh$_2$). IR (CO, cm^{-1}): 2036 s, 1982 s, 1956 vs, 1907 s (solid KBr).

Synthesis of (P−P)AuMn$_2$(CO)$_7$(μ-PPh$_2$) (2c). Similar preparation from Me$_3$NO (0.0278 g, 0.25 mmol), **1c** (0.0922 g, 0.05 mmol), and dppp (0.0206 g, 0.05 mmol) in THF (25 mL) at 50 °C for 6 h gave two bands: band 1 (orange, **1c**, 0.0120 g, 13%) and band 2 (red, **2c**, 0.0213 g, 20%), after elution with CH_2Cl_2/hexane (1:1). Anal. Calcd for **2c**: C, 50.20; H, 3.30. Found: C, 50.06; H, 3.19. ESMS: [**2c** + Na]$^+$ (*m*/*z* 1122.6); [**2c** − H]$^-$ (*m*/*z* 1099.1). ^{1}H NMR (δ): 2.14−2.17 (m, CH$_2$, 2H); 2.37−2.51 (m, CH$_2$, 2H); 3.33 (m, CH$_2$, 2H); 7.14−7.32 (m, Ph, 22H); 7.53−7.56 (m, Ph, 4H); 7.85−7.91 (m, Ph, 4H). ^{31}P NMR (δ): 61.35, 61.47 (d, $^4J_{PP}$ = 15 Hz, P$_{Au}$); 65.46 (s, br, P$_{Mn}$); 217.24 (s, br, PPh$_2$). IR (CO, cm^{-1}): 2033 s, 1985 s, 1958 s, 1941 s, 1912 s, 1902 s, 1893 s (solid KBr).

Synthesis of (P−P)AuMn$_2$(CO)$_7$(μ-PPh$_2$) (2d). Similar preparation from Me$_3$NO (0.0231 g, 0.21 mmol), **1d** (0.0916 g,

(13) *SMART & SAINT Software Reference Manuals*, Version 4.0; Siemens Energy & Automation, Inc., Analytical Instrumentation: Madison, WI, 1996.
(14) Sheldrick, G. M. *SADABS, a software for empirical absorption correction*; University of Göttingen: Göttingen, Germany, 1996.
(15) *SHELXTL Reference Manual*, Version 5.03; Siemens Energy & Automation, Inc., Analytical Instrumentation: Madison, WI, 1996.

0.05 mmol), and dppe (0.0204 g, 0.05 mmol) in THF (50 mL) at 80 °C for 5 h gave two bands: band 1 (orange, **1d**, 0.0138 g, 15%) and band 2 (red, **2d**·1/4CH_2Cl_2, 0.0091 g, 8%). There were brown uncharacterizable decomposition products deposited at the baseline upon elution. When the reaction was carried out at lower temperatures, such decomposition products were reduced, but the yield of **2d** was also reduced to trace level. Anal. Calcd for **2d**·1/4CH_2Cl_2: C, 49.06; H, 3.14. Found: C, 48.61; H, 3.02. ESMS: [**2d** + Na]$^+$ (*m*/*z* 1108.5). ^{1}H NMR (δ): 2.44 (s, CH_2, 2H); 2.93, 3.01 (d, CH_2, 2H, $^2J_{H-P}$ = 24.50 Hz); 5.29 (s, CH_2Cl_2, 0.5H); 7.36 (m, Ph, 22H); 7.66 (m, Ph, 4H); 7.80−7.86 (m, Ph, 4H). ^{31}P NMR (δ): 56.70, 57.05 (d, $^3J_{PP}$ = 42 Hz, P_{Au}); 69.17, 69.45 (d, br, $^3J_{PP}$ = 34 Hz P_{Mn}); 221.17 (s, br, PPh_2). IR (CO, cm^{-1}): 2033 s, 1996 s, 1987 s, 1964 s, 1936 s, 1913 vs (solid KBr).

Synthesis of (P−P)AuMn$_2$(CO)$_7$(μ-PPh$_2$) (2e). Similar preparation from Me_3NO (0.0278 g, 0.25 mmol), **1e** (0.0908 g, 0.05 mmol), and dppm (0.0192 g, 0.05 mmol) in THF (50 mL) at 60 °C for 12 h gave two bands: band 1 (orange, **1e**, 0.0088 g, 10%) and band 2 (red, **2e**, 0.0034 g, 3%). Similar brown uncharacterizable decomposition products were also found at the baseline. Anal. Calcd for **2e**: C, 49.28; H, 3.01. Found: C, 49.25; H, 3.20. ESMS: [**2e** − H]$^-$ (*m*/*z* 1071.0). ^{1}H NMR (δ): 3.58 (t, CH_2, 2H, $^2J_{H-P}$ = 9.07 Hz); 7.21−7.36 (m, Ph, 22H); 7.56 (m, Ph, 4H); 7.88−7.94 (m, Ph, 4H). ^{31}P NMR (δ): 65.90, 66.91 (d, $^2J_{PP}$ = 122 Hz, P_{Au}); 82.83, 83.87 (d, br, $^2J_{PP}$ = 126 Hz P_{Mn}); 199.44 (s, br, PPh_2). IR (CO, cm^{-1}): 2032 s, 1986 s, 1954 vs, 1905 vs (solid KBr).

Acknowledgment. The authors acknowledge the National University of Singapore (NUS) for financial support (RP143-000-013-112). Technical support from the Department of Chemistry of NUS is greatly appreciated. We specially thank Dr. Vittal J. J. and Miss Tan Y. K. for their help in obtaining the crystallographic data, and Mdm Chen Lijun for obtaining the ESMS spectra.

Supporting Information Available: A listing of tables giving crystal and structure refinement data, atomic coordinates and equivalent isotropic displacement parameters, bond lengths and bond angles, anisotropic displacement parameters, and hydrogen coordinates and isotropic displacement parameters for **2c**, **2d**, and **2a**. This material is available free of charge via the Internet at http://pubs.acs.org. CIF files are also available via the Internet.

OM0100434